Homogeneous Ruthenium-Catalyzed Acrylate Dimerization. Isolation, Characterization, and Crystal Structure of the Catalytic Precursor Bis(dimethyl muconate)-(trimethyl phosphite)ruthenium(0)†

Ronald J. McKinney* and Mitchell C. Colton

Central Research & Development Department, Experimental Station, E. I. du Pont de Nemours & Company, Wilmington, Delaware 19898

Received July 9, 1985

Reduction of $RuCl_3 \cdot 3H_2O$ with Zn/MeOH in the presence of methyl acrylate generates a catalytic system for the dimerization of alkyl acrylates to hexenedioates. Selectivity and rate are influenced by added phosphorus donor ligands, solvent, reducing agent, and Brønsted acids. The complex $(MUC)_2P(OMe)_3Ru^0$ (MUC = dimethyl muconate) has been isolated from a reduced catalyst mixture after treatment with $P(OMe)_3$ and the structure determined by low-temperature single-crystal X-ray diffraction methods. It crystallizes in an orthorhombic unit cell of symmetry *Pbca* (no. 61) with (at −100 °C) a = 14.390 (2) Å, b = 23.578 (3) Å, c = 13.501 (2) Å, V = 4581 (2) Å^3, and ρ(calcd) = 1.640 g cm^{-3} for Z = 8. Refinement converged at R = 0.049 and R_w = 0.041 for the 3309 independent diffractometry data collected with Mo Kα radiation ($4 < 2\theta < 50$) (number of variables refined = 405).

Introduction

The selective tail-to-tail coupling of functionally substituted olefins such as acrylates or acrylonitrile offers interesting possibilities for the synthesis of fine chemicals and industrially important large scale polymer intermediates. Electrolytic hydrodimerization of acrylonitrile to adiponitrile (a nylon intermediate) is currently practiced on a large scale.[1] We have examined the dimerization of methyl acrylate (MA) with a view to its use in the synthesis of adipic acid (another nylon intermediate)[2] and as an intermediate step in fine chemical syntheses of pharmaceutical interest.[3]

Alderson, Jenner, and Lindsey[4] reported in 1965 that both ruthenium and rhodium salts would catalyze the selective dimerization of methyl acrylate (MA) to dimethyl hexenedioate (DHD) at elevated temperature (210 and 150 °C, respectively). Shortly thereafter, Haszeldine and coworkers[5] reported that palladium salts also catalyze the linear dimerization and most subsequent work has focused on the palladium system because of the very high selectivity. However, the palladium system suffers from a very short catalyst lifetime due to the precipitation of palladium metal. The catalyst lifetime may be prolonged by adding oxidants which regenerate the active Pd(II).[6] However, this is impractical for any large scale utility. On the other hand, whereas the ruthenium-catalyzed reaction was reported to be less selective, higher conversion suggested that catalyst utility may not be a problem.[4] There have been numerous studies of hydrodimerization of acrylonitrile using ruthenium catalysts in the presence of hydrogen, and some of these have referred to similar reactions with MA.[7] However, they have all suffered from the coproduction of methyl propionate through hydrogenation of MA. We have therefore carried out our studies in the absence of hydrogen and as such generate dimers and trimers of MA which are unsaturated.

Considering the moderate conditions necessary for catalyzing MA dimerization with palladium, it was our hypothesis that the high temperatures reported for ruthenium catalysis (and perhaps in some cases the need for hydrogen) reflected a need to reduce Ru(III) to some lower oxidation state. We therefore began our studies with a precatalysis chemical reduction of $RuCl_3 \cdot 3H_2O$.

Results and Discussion

Upon treating $RuCl_3 \cdot 3H_2O$ with Zn powder in the presence of methyl acrylate (MA) and methanol at ambient temperature, the deep brown mixture passes through a blue-green stage and then lightens to an amber color. Gas chromatographic analysis at this stage reveals the presence of a small amount of dimethyl hexenedioate (DHD), dimethyl 2-methylpentenedioate (MPD), methyl propionate (MPR), and dimethyl muconate (MUC) (the doubly unsaturated C6 dioate) (eq 1). No further production of

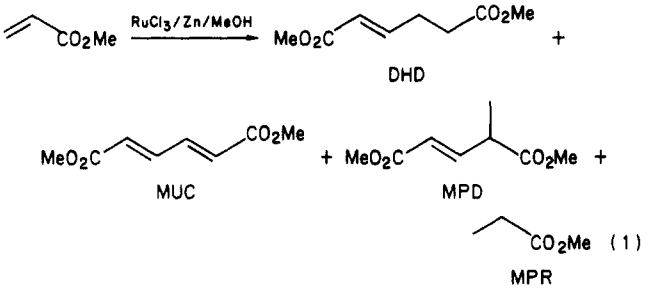

(1)

coupling products occurs at ambient temperature after the amber coloration is achieved. If methanol is omitted from the mixture, no color change occurs and no coupling products are detected. Separation of Zn from the mixture and heating of the solution in a sealed glass vessel for 16 h at 125 °C results in approximately 30% conversion of MA to dimers (including DHD, MPD, and MUC) and trimers (unknown structure). This approaches the conversion reported by Alderson at 210 °C in a similar length of time.

Several other metal powders were found to be moderately activating (Table I). These include manganese, iron,

† Contribution No. 3756.

(1) Baizer, M. H. *Chemtech* **1980**, 161-164. Danly, D. E. *Chemtech* **1980**, 302-311.
(2) McKinney, R. J. U.S. Patent 4 504 674, 1985.
(3) Nugent, W. A.; Hobbs, F. W. *J. Org. Chem.* **1983**, *48*, 5364-5366.
(4) Alderson, T.; Jenner, E. L.; Lindsey, R. V. *J. Am. Chem. Soc.* **1965**, *87*, 5638; Alderson, T., U.S. Patent 3 013 066, 1961.
(5) Barlow, M. G.; Bryant, M. J.; Haszeldine, R. N.; Mackie, A. G. *J. Organomet. Chem.* **1970**, *21*, 215.
(6) Pracejus, H.; Krause, H.-J.; Oehme, G. *Z. Chem.* **1980**, *20*, 24.
(7) For example see: Cornforth, D. A.; Waddan, D. Y.; Williams, D. *Canadian* Patent 796 775, 1968.

0276-7333/86/2305-1080$01.50/0

Table I. Reducing Agents

reducing agent[a]	reductn potential,[b] eV	dimer,[c] mol/Ru
none		1
Ni	0.2	1
Co	0.3	5
Cu	0.3	6
Fe	0.4	6
Cr	0.7	2
Zn	0.8	24
Mn	1.0	6
V	1.2	1
Ti	1.6	2
Al	1.7	2

[a] Powdered metals. [b] Vs. H^+/H_2 under basic conditions (*CRC Handbook*, 57th ed.; CRC Press: Cleveland, OH, 1900). [c] $[RuCl_3]$ = 0.035 M; MeOH/MA = 1/12; at 140 °C for 3 h.

Table II. Summary of X-ray Diffraction Results of 1a

formula	$C_{19}H_{29}O_{11}PRu$
fw	565.48
cryst system	orthorhombic
space group	*Pbca*, no. 61
unit cell	
temp, °C	−100
a, Å	14.390 (2)
b, Å	23.578 (3)
c, Å	13.501 (2)
V, Å^3	4581 (2)
Z	8
P(calcd), g cm^{-3}	1.640
cryst dimens, mm	0.26 × 0.15 × 0.25
no. of indepdent reflctns	5267
no. of reflctns $F_o^2 > \eta\sigma(F_o^2)$	3309
no. of variable refined	405
R	0.049
R_w	0.041
largest peaks in final difference Fourier, e A^{-3}	0.85 and 0.75 near Ru

cobalt, and copper. However, none of these approached the activating ability of zinc. It is interesting that titanium, vanadium, chromium, nickel, and aluminum did not show any activation. However, nickel may not have sufficient reducing capability whereas for the others, no attempt was made to remove oxide coatings of the metal powders which could be expected to diminish their reactivity. Tributyltin hydride was also unsuccessful as an activator.

Isolation of Ru(0) Complex. When $RuCl_3 \cdot 3H_2O$ in methanol is treated with zinc powder in the presence of MA, a color change as described above occurs. Addition of excess $P(OMe)_3$ causes a further lightening of the color to a deep yellow. Removal of excess methanol and MA under vacuum followed by extraction and recrystallization results in pale yellow crystals of **1a**. The infrared spectrum reveals a carbonyl stretching frequency at ν_{CO} 1710 cm^{-1} characteristic of an ester carbonyl unit. The proton NMR spectrum shows resonances at δ 1.2 (dd, 4, J = 11, 7 Hz, $CHCHCO_2Me$), 3.5 (s, 12, CO_2Me), 3.65 (d, 9, J = 11 Hz, $P(OMe)_3$), and 5.25 (dd, 4, J = 3, 7 Hz, $CHCHCO_2Me$) consistent with two coordinated MUC ligands for each $P(OMe)_3$.[8c] A single-crystal X-ray diffraction study confirmed this assignment. Pertinent crystallographic data may be found in Table II, and selected bond distances and angles are given in Table III. The structure, illustrated in Figure 1, is best described as a square pyramid with α carbons of the muconate ligands (C12, C15, C22, C25) defining the base and the phosphorus at the apex of the square pyramid. The ruthenium atom lies essentially in the base plane. The structure is very similar to those of several bis(butadiene) complexes and muconate complexes which have recently been structurally characterized.[8]

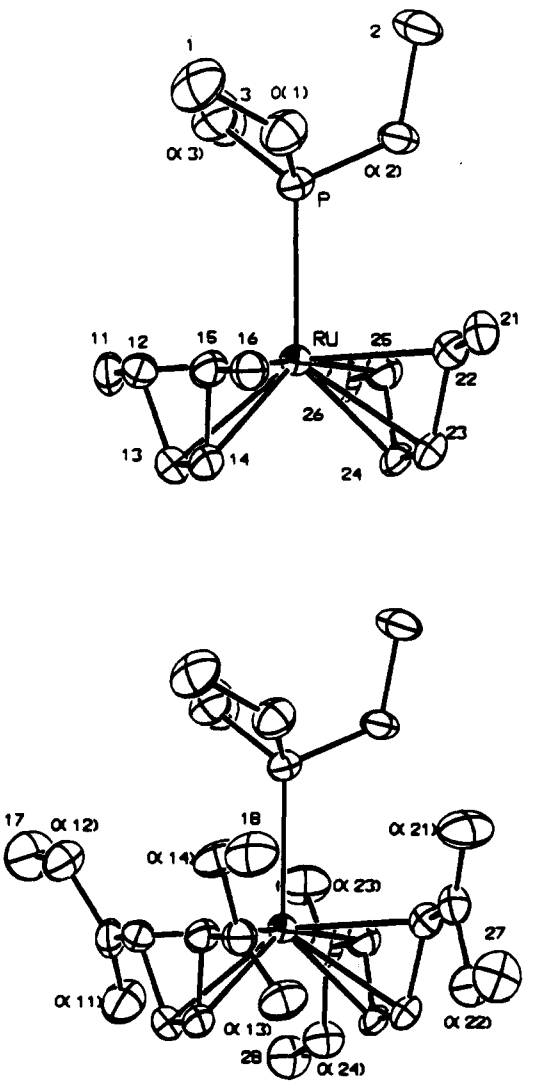

Figure 1. Structure of molecule **1a**. Lower view includes all non-hydrogen atoms. Upper view excludes oxygen and methyl atoms from the carbomethoxy groups of the muconate ligands for a clearer view of the coordination sphere.

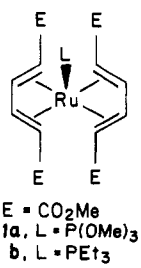

E = CO_2Me
1a, L = $P(OMe)_3$
b, L = PEt_3

Treatment of a catalyst mixture with PEt_3 results in the isolation of a complex the spectroscopic and analytical data of which are consistent with a similar structure **1b**, where PEt_3 replaces the $P(OMe)_3$ ligand. An attempt to isolate a complex with a more labile ligand in the apical position, i.e., acetonitrile resulted in a yellow solid in which the proton NMR spectrum is consistent with coordinated MUC and a nonstoichiometric amount of acetonitrile. Treatment of this complex with $P(OMe)_3$ causes a rapid and quantitative conversion to complex **1a**.

(8) (a) Harlow, R. L.; Krusic, P. J.; McKinney, R. J.; Wreford, S. S. *Organometallics* **1982**, *1*, 1506. (b) Huttner, G.; Neugebauer, D.; Razavi, A. *Angew. Chem.* **1975**, *87*, 353. c) DePaoli, M. A.; Frühauf, A.-W.; Grevels, F.-W.; Koerner Von Gustoaf, E. A.; Riemer, W.; Kruger, C. *J. Organomet. Chem.* **1977**, *136*, 219.

Table III. Selected Bond Distances (Å) and Bond Angles (deg) with Estimated Standard Deviations

Bond Distances			
Ru-P	2.325 (1)	C(21)-C(22)	1.461 (6)
Ru-C(12)	2.226 (5)	C(22)-C(23)	1.423 (6)
Ru-C(13)	2.154 (4)	C(23)-C(24)	1.406 (6)
Ru-C(14)	2.155 (5)	C(24-C(25)	1.398 (6)
Ru-C(15)	2.240 (5)	C(25)-C(26)	1.476 (6)
Ru-C(22)	2.220 (5)	C(21)-O(21)	1.204 (5)
Ru-C(23)	2.178 (5)	C(21)-O(22)	1.354 (6)
Ru-C(24)	2.164 (4)	O(22)-C(27)	1.443 (7)
Ru-C(25)	2.235 (5)	C(26)-O(23)	1.198 (5)
		C(26)-O(24)	1.354 (5)
		O(24)-C(28)	1.455 (5)
C(11)-C(12)	1.468 (7)		
C(12)-C(12)	1.426 (6)		
C(13)-C(14)	1.392 (7)	P-O(1)	1.604 (3)
C(14)-C(15)	1.415 (7)	P-O(2)	1.584 (3)
C(15)-C(16)	1.462 (6)	P-O(3)	1.579 (3)
C(11)-O(11)	1.212 (5)	O(1)-C(1)	1.406 (6)
C(11)-O(12)	1.344 (5)	O(2)-C(2)	1.456 (6)
O(12)-C(17)	1.437 (6)	O(3)-C(3)	1.461 (7)
C(16)-O(13)	1.204 (5)		
C(16)-O(14)	1.344 (5)		
O(14)-C(18)	1.426 (7)		
Bond Angles			
C(11)-C(12)-C(13)	116.6 (4)	C(22)-C(21)-O(22)	113.0 (4)
C(12)-C(12)-C(14)	117.6 (4)	C(21)-O(22)-C(27)	116.2 (4)
C(13)-C(14)-C(15)	120.5 (5)	C(25)-C(26)-O(23)	127.0 (5)
C(14)-C(15)-C(16)	118.4 (4)	C(25)-C(26)-O(24)	110.6 (4)
C(12)-C(11)-O(11)	126.5 (5)	C(26)-O(24)-C(28)	116.1 (4)
C(12)-C(11)-O(11)	126.5 (5)	C(13)-Ru-P	129.0 (1)
C(11)-O(12)-C(17)	116.6 (4)	C(14)-Ru-P	128.1 (1)
C(15)-C(16)-O(13)	125.8 (4)	C(23)-Ru-P	122.7 (1)
C(15)-C(16)-O(14)	111.9 (4)	C(24)-Ru-P	126.6 (1)
C(16)-O(14)-C(18)	115.9 (4)	Ru-P-O(1)	114.8 (1)
C(21)-C(22)-C(23)	121.4 (5)	Ru-P-O(2)	112.0 (1)
C(22)-C(23)-C(24)	117.4 (4)	Ru-P-O(3)	122.1 (1)
C(23)-C(24)-C(25)	120.8 (4)	P-O(1)-C(1)	126.4 (4)
C(24)-C(25)-C(26)	120.6 (4)	P-O(2)-C(2)	121.4 (4)
C(22)-C(21)-O(21)	125.0 (5)	P-O(3)-C(3)	118.6 (4)

It is interesting that the MUC ligands are not easily displaced. Addition of several equivalents of $P(OMe)_3$ to an NMR sample of **1a** does not displace muconate ligand even upon warming to 50 °C.

Intuitively, one might not expect the oxidative-coupling product MUC to form in a reducing environment such as the zinc and methanol provide. We speculate that the sequence shown in Scheme I may account for the formation of MUC. Zinc and alcohol have been used for many years in the reduction of transition-metal salts; reduction proceeds by elimination of HCl and formaldehyde from an intermediate Cl-M-OCH_3 species and the HCl is scavenged by zinc metal. The presence of a good electron-withdrawing olefin such as MA would be expected to aid the reduction process by stabilizing the reduced metal through complexation. The tautomerism between a π-bonded olefin and a vinyl-hydride species illustrated in the second step has previously been demonstrated for olefin complexes of ruthenium[9] and implicated in hydrodimerization of acrylonitrile.[10] In fact the vinyl-hydride tautomer is the preferred form for the complex L_3Ru(MMA) where L = PPh_3 and MMA = methyl methacrylate.[11] The insertion of MA into the ruthenium-hydride bond to give a Ru-alkyl with the carboalkoxy group on the β-carbon has also been observed.[12]

Scheme I

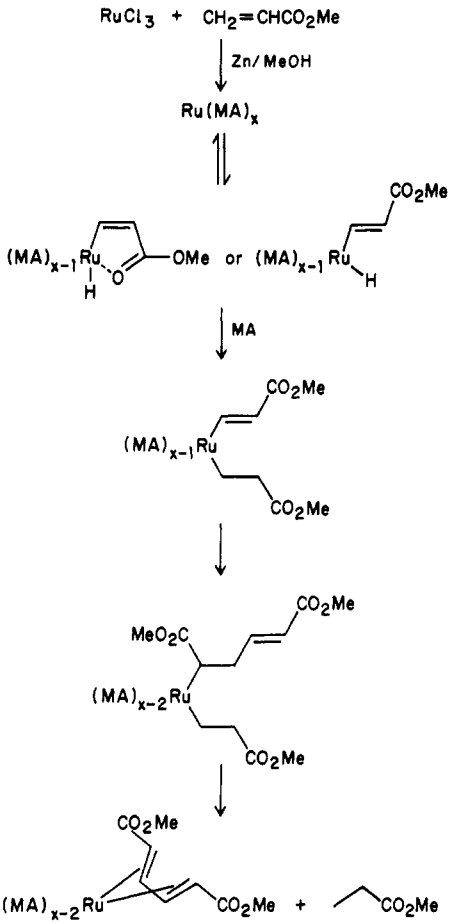

Reductive elimination of the vinyl and alkyl groups would provide an acceptable catalytic route to DHD, and indeed this has been proposed as a catalytic step in MA dimerization with palladium catalyst (eq 2).[13] However, the same workers have demonstrated that the Pd-vinyl bond readily inserts MA and, after β-hydride elimination, produces MUC (eq 3).[13] Other workers have observed that

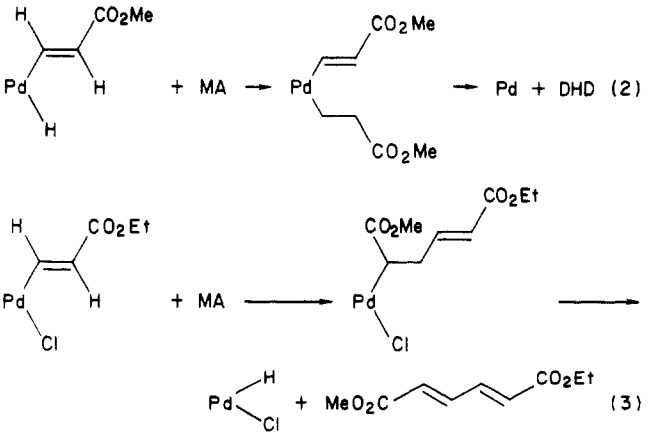

insertion of ethylene into a nickel-vinyl bond leads to butadiene.[14] It is therefore not unreasonable to expect such an insertion to be competitive with reductive elimination. Finally, we propose that the β-hydride elimination which produces MUC in the last step also produces methyl propionate (MPR) through reductive elimination of the

(9) Komiya, S.; Yamamoto, A. *Bull. Chem. Soc. Jpn.* **1976**, *49*, 2553.
(10) Billig, E.; Strow, C. B.; Pruett, R. L. *J. Chem. Soc., Chem. Comm.* **1968**, 1307.
(11) Komiya, S.; Ito, T.; Cowie, M.; Yamamoto, A.; Ibers, J. A. *J. Am. Chem. Soc.* **1976**, *98*, 3874.
(12) Gopinathan, S.; Joseph, K.; Gopinathan, C. *J. Organomet. Chem.* **1984**, *269*, 273.
(13) Oehme, G.; Pracejus, H. *J. Prakt. Chemie* **1980**, *322*, 798.
(14) Lehmkuhl, H.; Naydowski, C. *J. Organomet. Chem.* **1984**, *277*, C18.

Table IV. Solvent Effects[a]

solv	dimer,[b] mol/Ru (lin/br)	trimer, mol/Ru
toluene	46 (0.6)	1
ethyl acetate	85 (0.6)	2
tetrahydrofuran	49 (0.6)	3
pyridine	47 (0.1)	0
2-butanone	28 (0.6)	2
dimethylformamide	77 (3)	4
N-methylpyrrolidone	100 (16)	5
acetonitrile	22 (0.6)	3
dimethyl sulfoxide	27 (0.1)	0

[a] $[RuCl_3]$ = 0.0067 M; MeOH/MA/solvent = 1/25/50; $[P(i\text{-}Pr)_3]$ = 0.010 M; at 130 °C for 4 h. [b] Ratio of linear dimer (DHD) to branched dimer (MPD).

intermediate alkyl hydride. A repeat of this type of sequence would then produce the second muconate ligand.

The two complexes **1a** and **1b** were found to be catalysts for the dimerization of MA at 125 °C without further treatment. Whereas **1a** is equivalent to the corresponding in situ preparation, **1b** is somewhat less selective and active. The major difference between the use of the isolated catalyst and the in situ preparation is the presence of $ZnCl_2$ in the latter. Indeed, we have found that the presence of $ZnCl_2$ does effect rate and selectivity in the presence of phosphines but has no effect in the presence of phosphites or in the absence of phosphorus ligands altogether. The complex $(\eta^6\text{-}C_6H_6)(\eta^4\text{-}C_6H_8)Ru^0$ was also found to be active as a catalyst above 100 °C. Catalytic acrylate dimerization utilizing isolated zerovalent ruthenium complexes will be the subject of future publications.

Effect of Additives. In order to determine the scope of this catalytic system, we carried a series of scouting reactions exploring the effects of various additives.

In general, phosphorus donor ligands are moderately activating to the system with activation increasing in the order $P(OR)_3 < PAr_3 < PR_3$. $P(OAr)_3$ is somewhat deactivating. The optimum amount of ligand appears to correspond to a PR_3:Ru ratio of about 1.5:1. Increasing the amount of PR_3 results in increased amounts of the branched dimer dimethyl methyleneglutarate (DMG) (eq 4).[15] In these reactions, dimer formation is essentially

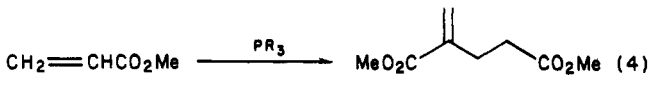

nonselective between linear dimers (DHD) and branched dimers (MPD), with ratios of DHD:MPD ranging from 3:1 to 1:1.

Solvent variation has a striking effect on selectivity and to a lesser extent on activity. Table IV compares product formation for a variety of solvents using a zinc and $P(i\text{-}C_3H_7)_3$ treated Ru catalyst system. Whereas activity, as qualitatively measured by total dimer product formed in 4 h at 130 °C, increases fourfold on changing from dimethyl sulfoxide to *N*-methylpyrrolidone (NMP), the proportion of linear (DHD) to branched dimer (MPD) increases from about 10% to 94%. In the case of pyridine and dimethyl sulfoxide, it appears that primarily dimer arising from PR_3 catalysis; i.e., DMG is formed (eq 4).

The presence of large amounts of methanol is unnecessary for catalyst activity and is actually detrimental to selectivity. We have found that only a few equivalents of methanol per $RuCl_3$ is necessary for zinc treatment activation. Increasing the amount of methanol results in increased amounts of the byproducts methyl propionate and methyl β-methoxy propionate. It is therefore desirable to keep the methanol content to a minimum.

Table V. Comparison of Additive Effects at 140 °C

cat.	dimer,[a] mol/Ru (lin/br)	trimer, mol/Ru
A[b]	3 (1)	<1
A + $P(i\text{-}Pr)_3$	1	0
A + Zn	29 (1)	6
A + Zn + $P(i\text{-}Pr)_3$	61 (1)	5
$RuCl_3$ + Zn + NMP[c]	117 (16)	14
$RuCl_3$ + Zn + $P(i\text{-}Pr)_3$ + NMP[c]	117 (19)	13
$RuCl_3$ + Zn + $P(i\text{-}Pr)_3$ + NMP[d]	87 (49)	4

[a] Ratio of linear dimer (DHD) to branched dimer (MPD). [b] Aldersons catalyst = $[RuCl_3]$ = 0.038 M; MeOH/MA = 25/75; at 140 °C for 3 h. [c] $[RuCl_3]$ = 0.006 25 M; MeOH/MA/NMP = 1/30/50; at 140 °C for 3 h. [d] $[RuCl_3]$ = 0.010 M; MeOH/MA/NMP = 1/25/25; at 130 °C for 3 h.

The addition of a variety of protic acids was found to be detrimental, and for most of the stronger acids, e.g., H_2SO_4, dimerization was completely inhibited. One remarkable exception was the addition of $HBF_4\cdot Et_2O$ to the catalyst zinc treated $RuCl_3\cdot 3H_2O/P(i\text{-}C_3H_7)_3$ in NMP; a very large increase in dimerization activity was noted but the product is 70% branched dimer (MPD). We did not observe such activation for any other solvent and phosphine combination, but the result is reproducible.

A comparison, of the effects of selected additives against the catalyst originally described by Alderson et al., is given in Table V. In the first four entries, the system is very similar to Alderson's and contains a large amount of methanol (25%). The last three entries contain very little methanol, and the MA content is more dilute because of the added solvent. (The last entry is similar to the penultimate entry except carried out at a lower temperature (130 °C), demonstrating the increased selectivity at lower temperatures.) However, the qualitative effects of the additives is readily apparent.

Whereas a detailed kinetic study has not been undertaken for this catalyst system, variation of MA and Ru concentrations suggest that the rate of dimer formation (DHD and MPD) is first order in Ru concentration and independent of the MA concentration (over an admittedly concentrated range, [MA] = 2–6 M). Apparently MA coordination is much more rapid than dimer formation and/or elimination from the catalyst. This may simply reflect that besides the one to two phosphines per Ru in the system, there are no better ligands than the MA. The rate of trimer formation appears to depend on the DHD concentration which is consistent with DHD being a weaker ligand. A typical product concentration vs. time plot is illustrated in Figure 2. The theoretical lines are derived by using the simple model encompassed by eq 5–8

$$Ru \rightarrow Ru' + DHD \quad (5)$$

$$Ru' + 2MA \rightarrow Ru \quad (6)$$

$$Ru + DHD \rightarrow Ru'' + trimer \quad (7)$$

$$Ru'' + MA \rightarrow Ru \quad (8)$$

in an iterative kinetic modeling computer program, GIT, which combines statistical comparison of experimental data with a GEAR generated theoretical model.[16] Rate constants for eq 6 and 8 were fixed at very high rates, and those of eq 5 and 7 were allowed to vary to fit the data.

(15) Rauhut, M. M.; Currier, H. U.S. Patent 3 074 999, 1963.

(16) Weigert, F. J., private communication. An iterative procedure is attached to a modified version of HAVCHEM obtained from: Stabler, R. N.; Chesnick, J. *Int. J. Chem. Kinet.* **1978**, *10*, 461.

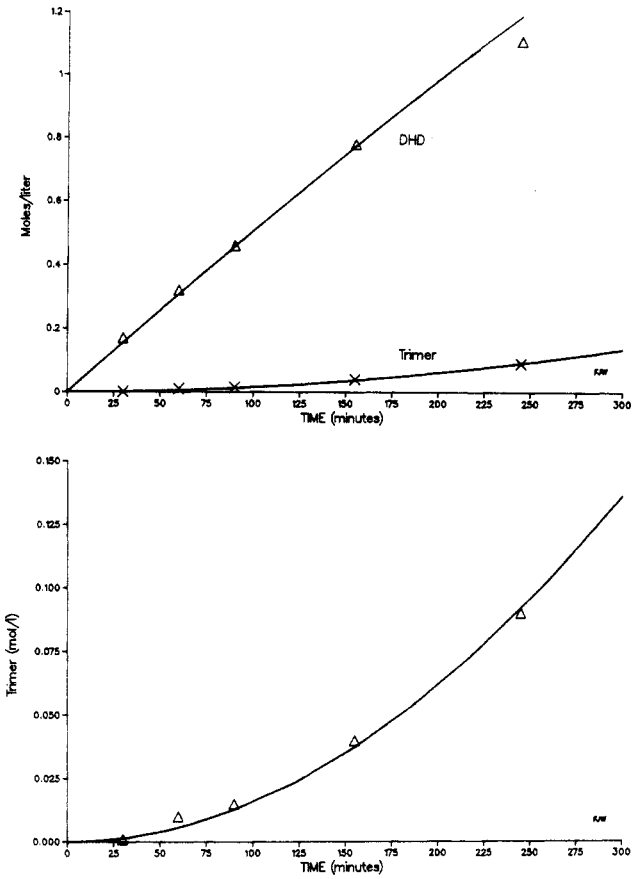

Figure 2. Production of dimethyl hexenedioate (DHD) and trimer (of MA) with time. Upper plot shows both DHD and trimer whereas lower plot shows only trimer (y axis expansion) to illustrate dependence on DHD concentration. Conditions: [Ru] = 0.010 M, [MA] = 5.3 M; [P(i-C_3H_7)$_3$] = 0.015 M in N-methylpyrrolidone at 130 °C. Prepared as described in "Typical Catalyst Preparation" in Experimental Section.

Using this simple model, we have explored the relative rate effects of various phosphorus ligands. We find systematic changes in rate of dimerization which appear to correlate with electronic rather than steric factors of the phosphines and phosphites. Figure 3 illustrates rate changes in a limited series of alkyl phosphines which could result from either steric (Tolman's cone angles)[17] or electronic changes in the phosphine. However, when triphenylphosphine and alkyl and aromatic phosphites are included, the cone angle correlation breaks down. However, Tolman also noted that electronic changes in phosphorus ligands could be characterized by the infrared carbonyl stretching frequency (ν_{CO}) of the series of complexes Ni(CO)$_3$L where L is the phosphorus ligand.[17] Acknowledging that stretching frequencies may be very different on ruthenium, we nevertheless find a good correlation between Tolman's ν_{CO} values for phosphorus ligands and the logarithm of the relative rate constant as illustrated in Figure 4. Whereas this observation strongly suggests that the rate changes are derived from electronic rather than steric factors, the meaning of this correlation is under further investigation.

The mechanistic details at the molecular level remain unclear. However, the involvement of vinyl–hydride intermediates for olefin dimerizations as well as other carbon–carbon coupling procedures is gaining increasing support (ref 9, 10, 14, and 18), and in light of the isolation of **1**, we tend to favor a mechanism related to Scheme I.

(17) Tolman, C. A. *J. Am. Chem. Soc.* **1970**, *92*, 2953.
(18) Nubel, P. O.; Brown, T. L. *J. Am. Chem. Soc.* **1984**, *106*, 3474.

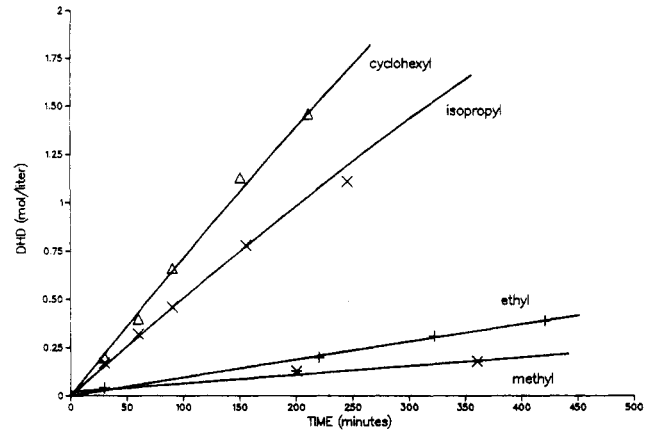

Figure 3. Comparison of rate of production of DHD using different trialkylphosphines, PR_3. Labels indicate R groups. Conditions similar to that described in "Typical Catalyst Preparation" in Experimental Section: R = cyclohexyl, k_5 = 0.73 min^{-1}; R = isopropyl, k_5 = 0.54 min^{-1}; R = ethyl, k_5 = 0.098 min^{-1}; R = methyl, k_5 = 0.046 min^{-1} (k_5 is the optimized rate constant for eq 5; see text).

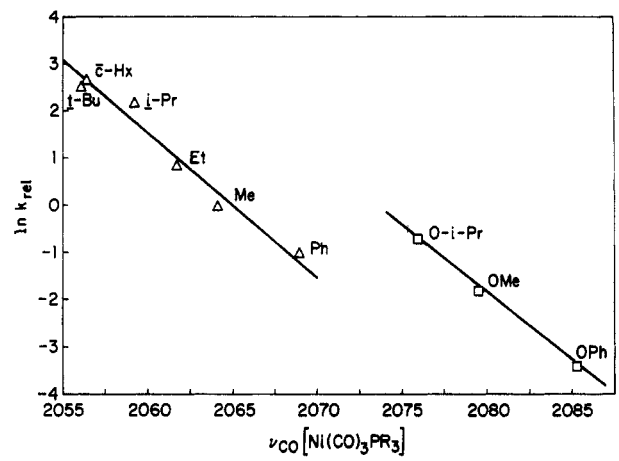

Figure 4. Plot of ln k_{rel} vs. ν_{CO} where k_{rel} are the relative rate constants of eq 5 (see text) when different phosphines PR_3 are utilized in the dimerization of MA with $RuCl_3$ (k_{rel} = 1 for PMe_3). ν_{CO} (A_1) for Ni(CO)$_3$PR$_3$ are from ref. 17.

It is interesting to note that in the presence of phosphine ligands, little or no methyl propionate (MPR) is produced and trimer is the predominant higher oligomer. However, in the absence of phosphorus ligand, dehydrotrimer (trimer less two hydrogen atoms) is the major higher oligomer and about 1 equiv of MPR for each dehydrotrimer is produced. Separate experiments have shown that dimethyl muconate (MUC) reacts very rapidly with MA under catalytic conditions to produce dehydrotrimer. Therefore in the absence of phosphine, a sequence as illustrated in Scheme I could operate to produce MUC which then reacts with MA to produce dehydrotrimer. On the other hand, in the presence of phosphorus ligand, the last two steps of the scheme may be inhibited and dimerization may occur by reductive elimination from the vinyl–alkyl intermediate.

Experimental Section

All preparative manipulations were carried out under an atmosphere of nitrogen in a Vacuum/Atmosphere Corp. drybox. Reagents were used as received from vendors. Many of the catalytic mixtures were sealed by torch in heavy-walled glass ampules under vacuum at liquid-nitrogen temperatures and then submerged in a thermostated oil bath (±1 °C) for specified periods. The ampule was then cooled in an ambient-temperature water bath and opened to air, completely quenching the reaction. The quenched reaction mixtures were analyzed by gas chromatography [HP5710A, FID; column, 10% SE 30 on 80/90 mesh Anakrom

ABS, 12 ft × $^1/_8$ in. (Supelco)] and product concentrations calculated by applying appropriate response factors and comparing integrated area of products with that of the internal standard decane. Approximate response factors were determined by using dimethyl adipate and subsequently checked against a distilled sample of dimethyl hexenedioate isomer mixture. Identity of the products was determined by mass spectral analysis (GC–MS) and, in the case of isomers, by comparison of retention times against authentic samples of known isomers of dimethyl hexenedioate. The identity of the trimer fractions rests solely on mass spectral molecular weight determination.

Typical Catalyst Mixture Preparation. A catalyst solution was prepared by mixing $RuCl_3 \cdot 3H_2O$ (0.13 g, 0.5 mmol), methanol (1 cm^3), methyl acrylate (25 cm^3, 275 mmol), and excess powdered zinc for 0.5 h and filtering. The filtrate was treated with triisopropylphosphine (0.12 g, 0.75 mmol), *N*-methylpyrrolidone (25 cm^3), decane (1.00 cm^3), and hydroquinone (0.1 g) (polymerization inhibitor). Aliquots were sealed under vacuum and heated at 130 °C for various periods of time. Analysis by GC as indicated above leads to the product vs. time plot of Figure 2. Hydrogenation of one of the higher conversion samples (10% Pd/C in ethyl acetate, 20 °C, 20 psig) revealed that the dimer fraction was 98% linear (DHD).

A variety of other mixtures were made in a similar way with no added solvents, or solvents described in Table IV, and with or without a variety of other phosphines or phosphites.

Isolation of Ru(0) Complexes. Bis(dimethyl muconate)(trimethyl phosphite)ruthenium(0) (1a). $RuCl_3 \cdot 3H_2O$ (0.26 g, 1.0 mmol) was treated with methyl acrylate (5.0 cm^3) and excess powdered zinc in methanol (20 cm^3) at ambient temperature for 1 h. Trimethyl phosphite (0.37 g, 3.0 mmol) was added and the mixture stirred for a further 1 h and then filtered. Solvent was removed from the amber solution under reduced atmosphere to give a brown oil which was extracted with toluene. The toluene was removed from the yellow solution under reduced pressure and the residue extracted with hexane/diethyl ether. Upon reducing the volume of the solution and cooling to −30 °C, pale yellow crystals of **1a** formed and were isolated by filtration and dried under high vacuum (0.080 g).

Bis(dimethyl muconate)(triethylphosphine)ruthenium(0) (1b). $RuCl_3 \cdot 3H_2O$ (2.0 g, 7.6 mmol), methanol (70 cm^3), methyl acrylate (70 cm^3), and manganese powder (1.0 g) were stirred overnight. The mixture was filtered and stripped to a red oil. The red oil was redissolved in CH_3CN (25 cm^3), and then Et_2O (225 cm^3) was slowly added, causing an off-white precipitate to form which was separated by filtration (2.05 g vs. 2.4 g theory for $MnCl_2 \cdot 2CH_3CN$). The filtrate was treated with excess triethylphosphine (2 cm^3) and the solution stripped to a dark oil which was redissolved in acetone. Decane was added, the volume reduced, and the solution cooled to −30 °C. Yellow crystals (**1b**, mp 156 °C) separated and were isolated by filtration: ^1H NMR (acetone-d_6) δ 1.15 (dd, 4, J = 6, 9 Hz), 1.3 (dt, 9, J = 7, 14 Hz), 2.6 (dq, 6, J = 7, 7 Hz), 3.65 (s, 12), 5.45 (m, 4). Anal. Calcd for $C_{22}H_{35}O_8PRu$ (mol wt 559): C, 47.23; H, 6.26. Found: C, 47.21; H, 6.42.

Crystal Structure of 1a. All of the crystallographic data were obtained by using a Syntex P3 diffractometer equipped with a graphite monochromator and a low-temperature system (Mo Kα radiation, λ = 0.71069 Å). The unit cell dimensions were refined from Bragg angles of 47 reflections which had 2θ values between 24° and 26°. Intensity data were collected by using Ω scan technique with a scan range of 1.0; backgrounds were measured at each end of the scan with Ω offset by 1.0. The intensities of the four standard reflections were monitored periodically; only statistical fluctuations were noted. Psi scans revealed intensity variation with psi, and thus an empirical absorption correction was made (transmission factors ranged from 0.89 to 1.00).

The structure of **1a** was refined by full-matrix least-squares techniques. All positional and thermal parameters (anisotropic for Ru, P, O, and C; isotropic for H) were included in the refinement.

A summary of the crystallographic results is given in Table II. The molecular geometry is detailed in Figure 1 and Table III. Other crystallographic information has been submitted as supplementary material. The mathematical and computational details of the computer software can be found elsewhere.[19]

Registry No. **1a**, 101200-02-6; **1b**, 101200-03-7; $RuCl_3$, 10049-08-8; Zn, 7440-66-6; DHD, 627-93-0; MPD, 14035-94-0; MPR, 554-12-1; MUC, 1733-37-5; Ni, 7440-02-0; Co, 7440-48-4; Cu, 7440-50-8; Fe, 7439-89-6; Cr, 7440-47-3; Mn, 7439-96-5; V, 7440-62-2; Ti, 7440-32-6; Al, 7429-90-5; methyl acrylate, 96-33-3.

Supplementary Material Available: Tables of final positional parameters (as fractional coordinates), thermal parameters, and structure factor amplitudes (observed and calculated) (21 pages). Ordering information is given on any current masthead page.

(19) Nugent, W. A.; Harlow, R. L. *Inorg. Chem.* **1979**, *18*, 2030.